

ENNOBLEMENT OF STAINLESS STEEL
STUDIED BY X-RAY PHOTOELECTRON SPECTROSCOPY

B. H. Olesen

Center for Biofilm Engineering, Montana State University
Bozeman, MT 59717-3980, USA and
Environmental Engineering Laboratory, Aalborg University
DK-9000 Aalborg, Denmark

R. Avci

Image and Chemical Analysis Laboratory
Department of Physics, Montana State University
Bozeman, MT 59717-0350, USA

Z. Lewandowski

Center for Biofilm Engineering
Engineering Research Center, Montana State University
Bozeman, MT 59717-3980, USA

ABSTRACT

Manganese oxides deposited by biofilms of *Leptothrix discophora* SP-6 on 316L stainless steel corrosion coupons increased the open circuit potential of the steel to values of +375 mV_{SCE}. XPS spectra of the deposits compared to spectra of different manganese containing minerals indicated that the deposits were composed of MnO₂. The redox reaction responsible for the potential change results in electron transfer from the metal substratum to the mineral deposit. To study the processes of manganese dioxide reduction, MnO₂ which had been electroplated on stainless steel was reduced electrochemically. The surface chemistry before and after reduction was analyzed by XPS. We demonstrated that the manganese dioxide deposited on stainless steel coupons can be reduced to Mn²⁺ by accepting two electrons from the metal. MnOOH was identified as an unstable intermediate product in this reaction. Consequently we hypothesize, that manganese dioxide microbially deposited on stainless steel surfaces can provide an efficient cathodic reaction and accelerate microbially influenced corrosion processes.

Keywords: manganese oxidizing bacteria (MOB), *Leptothrix discophora* SP-6, biofilm, mineral deposit, biomineralization, manganese dioxide, corrosion, ennoblement, 316L stainless steel, surface analysis, x-ray photoelectron spectroscopy (XPS), electron spectroscopy for chemical analyses (ESCA)

INTRODUCTION

Numerous experiments have indicated that microbial colonization can change the surface properties and affect the electrochemical behavior of metals. For the case of passive metals, a majority of the documented experiments refer to a phe-

Publication Right

Government work published by NACE International with permission of the author(s). Requests for permission to publish this manuscript in any form, in part or in whole must be made in writing to NACE International, Publications Division, P.O. Box 218340, Houston, Texas 77218-8340. The material presented and the views expressed in this paper are solely those of the author(s) and are not necessarily endorsed by the Association. Printed in the U.S.A.

nomenon called "ennoblement", in which the Open Circuit Potential (OCP) increases in the positive (noble) direction along with an increase in cathodic current.¹⁻⁹ The final OCP ranges from +200 mV_{SCE}² to +450 mV_{SCE}.^{1,4} Observed potentials are usually higher in freshwater than in seawater. Numerous explanations have been suggested to explain ennoblement: localized changes in pH near the surface³, formation of "a thin organic film" on the surface⁴, or production of passivating siderophores⁹, organo-metallic complexes², enzymes⁶, or extracellular substances¹ increasing the efficiency of the cathodic reactions.

Recent studies indicate that the mechanism of ennoblement includes biomineralization of manganese, which is consistent with documented cases of stainless steel failure. For example, elevated amounts of manganese deposits were reported in a case of pitting corrosion of turbine runner blades (G-X 5 CrNi 13 4 and X 3 CrNi 13 4) in a hydroelectric power plant in the Netherlands^{10,11}. Despite the fact that the selected material was able to resist pitting corrosion of existing chloride concentration (20-170 mg/L), the runner blades were severely damaged. OCP of the biological deposits scraped from the turbine runner blades was +570 mV_{SCE} at pH 7.5, 20°C and 0.1 mg/L Mn²⁺. Analysis of the deposit by Scanning Electron Microscopy (SEM) and X-ray Diffraction (XRD) revealed significant amounts of manganese containing minerals (25% w/w MnOOH and 8% w/w MnO₂). It was suggested that the potential of the deposit was due to reduction of manganese dioxide to divalent manganese (E₀' = +550 mV_{SCE} at pH 7.5, [Mn²⁺] = 0.1 mg/l). The investigation concluded that the massive pitting corrosion of the turbine runner blades was caused by the biomineralization of manganese. Another study demonstrated that 316L stainless steel ennobled in a fresh water stream^{12,13}, reaching +350 mV_{SCE} after 30 days of exposure. Significant amounts of manganese oxides were found within the biofilms. Laboratory simulation of the processes using the Manganese Oxidizing Bacterium (MOB) *Leptothrix discophora* SP-6 confirmed that the ennoblement was caused by the biomineralized manganese¹⁴. Reduction of manganese dioxide to manganese oxyhydroxide, MnOOH (E₀' = +335 mV_{SCE} at pH 8.0) was suggested as the reason for the potential shift.

Neither the chemical composition of the deposited manganese containing mineral, nor the electrochemical processes responsible for the ennoblement is clearly understood. Two issues will be addressed in this report: 1) the mineralogy of the biologically deposited manganese oxides, and 2) the mechanism of manganese dioxide reduction. To address the first issue, pure culture biofilms of MOB were grown on 316L stainless steel under laboratory conditions. The composition of the deposits was determined by comparing the XPS spectra of the deposits with the spectra of different manganese containing minerals. To address the second issue, we studied reduction of thin layers of manganese dioxide, electroplated on stainless steel corrosion coupons, by passing a small cathodic current. Surface analysis of the deposits after the electrochemical reduction provided information about the mechanism of manganese oxide reduction. The shift to an abiotic system was necessary to obtain a uniform mineral film and to eliminate charge transfer due to the biofilm itself.

EXPERIMENTAL METHODS

Sample preparation

Type 316L stainless steel corrosion coupons (1.6 cm diameter) were epoxy-embedded in polycarbonate holders and polished as previously described¹⁵. The composition of the steel is shown in Table 1. Adhesive copper tape was used to make electrical connections to the backs of the coupons. After polishing, the samples were sonicated in distilled water, then in 95% ethanol, then dried with a paper towel. All samples were left in contact with atmospheric air for 24 hours to form a passive film. Prior to the biological experiments the coupons were sterilized by soaking in 95% ethanol for one minute, followed by exposure to UV-light for 12 hours.

TABLE 1
ELEMENTAL COMPOSITION (WT. %) OF 316L STAINLESS STEEL
AS PROVIDED BY VENDOR.

Fe	Cr	Ni	Mo	Mn	Si	P	N	C	S
Bal.	16.19	10.19	2.10	1.71	0.39	0.034	0.03	0.017	0.001

Biological experiments

Cultures of *Leptothrix discophora* SP-6¹⁶ obtained from American Type Culture Collection (ATCC no. 51168) were grown in mineral-salt-pyruvate-vitamin (MSPV) medium (ATCC no. 1917). Subcultures were preserved by freezing at -70°C¹⁷. Prior to each experiment a frozen culture was thawed and incubated for 48 hours in 5 ml MSPV medium. One ml of this culture was transferred to 100 ml MSPV medium and incubated for 48 hours. Five ml of the second culture was used to

inoculate 500 ml MSPV medium containing 200 μM Mn(II)^{14} as MnSO_4 in a batch reactor. Ten corrosion coupons were placed face down through holes in the lid of the 1L polycarbonate reactor. A Saturated Calomel Electrode (SCE) was connected to the media through a 1% agar salt bridge containing 1 mM Na_2SO_4 . OCPs were measured hourly.

Surface analyses

Small-spot XPS was performed using an electron spectrometer (model PHI 5600 ci). A monochromatic $\text{Al K}\alpha$ X-ray source was used with aperture no. 4 (analyzing area 800 μm in diameter) in addition to pass energies of 93.9eV and 58.7eV for full and partial scans. Full scans in the range of 0-1000 eV and energy windows for Mn2p (632-672 eV), Mn3p (43-63 eV), and O1s (525-545 eV) were collected. Charge neutralization was necessary in some instances to account for charging of non-conducting samples. Five manganese-containing compounds were used as standards: Mn metal (99.98%), MnO_2 (99%), Mn_2O_3 (97%), Mn_3O_4 (99%) and MnO (99%). MnOOH was synthesized through the oxidation of manganese sulfate^{18,19} by adding 20.4 ml of 30% H_2O_2 to 1 L of 0.06 M MnSO_4 . Next, 300 ml of 0.2 M NH_3 was added, and the solution was heated to 95°C for 6 h. Finally, the mixture was filtered through a 0.4 μm polycarbonate filter, and the deposits were washed several times with hot distilled water prior to drying in desiccator at room temperature for two days.

Prior to XPS analysis, coupons were cleaned with distilled water, air dried, then mechanically removed from their holders. Epoxy residues were removed mechanically to eliminate interference at high vacuum. Coupons were kept separately in sealed, nitrogen filled vials for 24 hours prior to analysis. Peak fitting of the obtained spectra with asymmetrical Gaussian/Laurensian curves was performed using software accompanying the electron spectrometer. Table 2 includes the peak fitting results from the standard manganese minerals. The ratio between Gaussian and Laurensian curvature was in the range of 50-70%. Changing the value within this range did not affect the overall fitting result, so the parameter was left out. The most significant difference among the six minerals was found at the Mn3p peak. Therefore, the following discussion includes observations of this orbital only.

TABLE I
POSITION AND SHAPE PARAMETERS FOR THE MN3P ORBITAL PEAK
OBTAINED FROM XPS SPECTRA OF DIFFERENT MANGANESE-CONTAINING MINERALS.

Mineral	Mn metal	MnO_2	Mn_2O_3	Mn_3O_4	MnO	MnOOH
Position [eV]	47.37	49.55	48.65	48.13	48.02	49.13
Width [eV]	1.41	2.02	1.69	1.82	1.80	1.92
Tail length [eV]	15	12.0	12.8	12.2	11.8	10.4
Tail scale	1.52	0.78	1.42	1.59	1.65	1.42

Electrochemical measurements

Electrochemical measurements were conducted using an EG&G potentiostat model 273A. Stainless steel corrosion coupons were electroplated with manganese dioxide from 0.1 M Na_2SO_4 and 5 mM MnSO_4 at pH 6.5 and at room temperature. 30 mC/cm^2 was electroplated using an anodic current of 100 $\mu\text{A}/\text{cm}^2$, which corresponded to 13.5 $\mu\text{g}/\text{cm}^2$ of MnO_2 , equivalent to a 250 nm thick homogenous mineral film covering the surface. Calculations are based on the two electron transfer reaction (1).



The manganese-covered coupons were placed in 30 ml of 0.1 M Na_2SO_4 at pH 6.5, and a cathodic current of 2 $\mu\text{A}/\text{cm}^2$ was passed between the coupon and a graphite counter electrode. The uniform plating of the coupons yielded reproducible reduction potential curves which allowed for the termination of the process at any time to analyze the surface chemistry at pre-designed intervals. The concentration of dissolved manganese in the electrolyte was measured utilizing the formaldoxine method²⁰: 1.5 ml ammonia-formaldoxine reagent was added to 0.5 ml of each sample and standard, allowing 30 minutes for color development, then measuring the absorbance (450 nm).

RESULTS AND DISCUSSION

Ten 316L stainless steel corrosion coupons exposed to a culture of *Leptothrix discophora* SP-6 in a manganese-containing medium developed stable OCPs at +375(\pm 15) mV_{SCE} within seven days. These potentials agree well with our previously

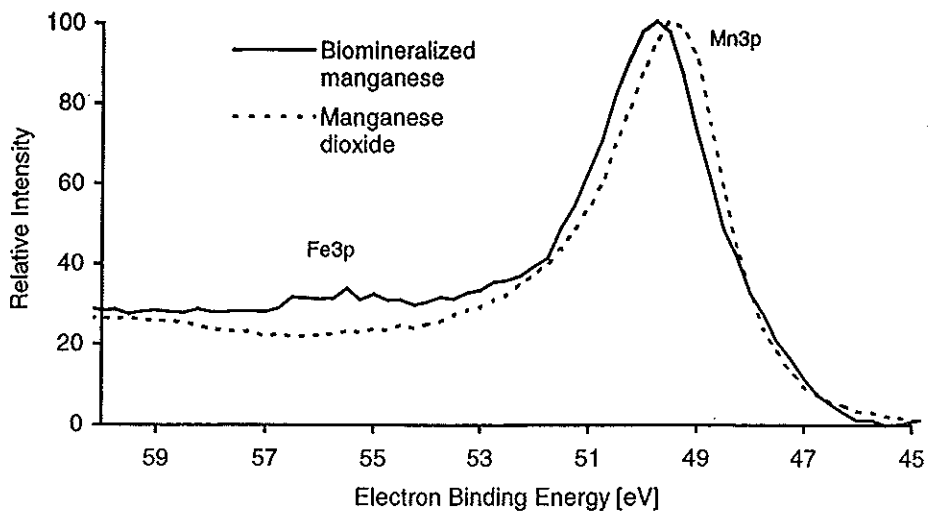


Figure 1. XPS spectra of biomineralized manganese and the manganese dioxide standard. Curves are individually scaled to equal height of Mn3p.

published results¹²⁻¹⁴. Potentials reported by Linhardt^{10,11} of manganese-rich deposits were considerably higher, around +570 mV_{SCE}. However, Linhardt^{10,11} measured the potentials of the deposits alone, whereas we measured potentials of the ennobled steel. We have shown previously¹⁴ that neither the presence of divalent manganese, nor the formation of an *L. discophora* SP-6 biofilm on the steel surface changes the OCP. The biomineralization of manganese oxides at the steel surface is solely responsible for the ennoblement. An XPS spectrum collected from one of the ennobled coupons along with the spectrum for manganese dioxide is shown in Figure 1. The spectra of biomineralized manganese could be fitted with a single peak: position 49.9 eV, width 2.5 eV, tail length 15, tail scale 0.3. from the spectra of different standard manganese minerals (Table 2), these values are indicative of manganese dioxide. The position for biomineralized manganese (49.9 eV) is slightly higher than the position for manganese dioxide (49.55 eV) which could mean that the valence of the present manganese atoms is higher than four. However manganese states with valences higher than four are only found in ionic species and are, except for the permanganate ion, stable only in highly alkaline solutions²¹. Based on these considerations, we conclude that the bacterium *Leptothrix discophora* SP-6 deposits manganese dioxide when grown in a medium containing divalent manganese.

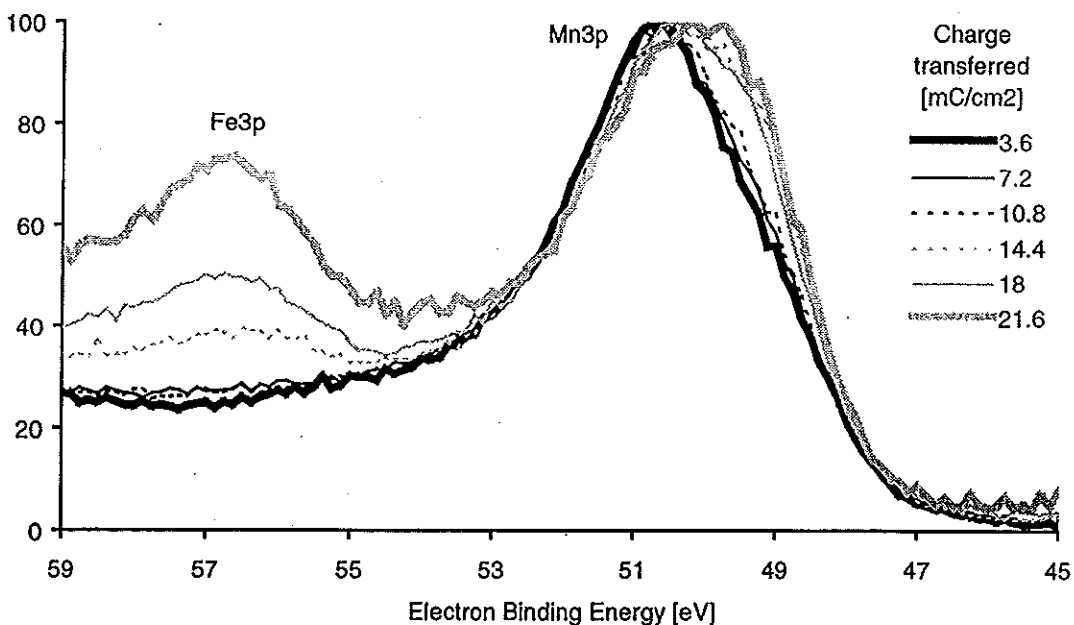


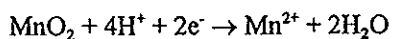
Figure 2. XPS spectra of reduced manganese dioxide film. Curves are individually scaled to equal height of Mn3p.

TABLE 3
POSITION AND SHAPE PARAMETERS FOR THE MN3P SPECTRA OF REDUCED MANGANESE DIOXIDE
ALONG WITH Mn^{2+} CONCENTRATIONS MEASURED IN THE ELECTROLYTE.

Sample ID	3.6	7.2	10.8	14.4	18	21.6	25.5	28.8	32.4
PEAK NO. 1 (MnO_2)									
Position [eV]	50.52	50.56	50.43	50.39	50.57	50.57	50.76	50.61	-
Width [eV]	2.19	2.18	2.08	2.08	1.90	1.95	1.64	2.0	-
Tail length [eV]	11.8	11.6	11.4	8.0	8.4	7.8	7.7	10.0	-
Tail scale	0.81	0.79	0.97	1.0	1.10	1.06	1.44	0.46	-
Area	31774	30276	26641	19054	20783	14837	8475	8515	-
% of total area	82.70	78.92	80.52	64.61	71.89	65.33	50.58	57.83	-
PEAK NO. 2 ($MnOOH$)									
Position [eV]	48.72	48.89	48.87	49.0	49.09	49.16	49.45	49.24	-
Width [eV]	1.61	1.61	1.61	1.61	1.91	1.78	2.03	1.86	-
Tail length [eV]	10.0	10.0	16.3	10.0	9.7	10.7	0.5	10.0	-
Tail scale	0.59	0.61	0.12	0.91	0.21	0.25	1.12	0.10	-
Area	6647	8087	6447	10439	8110	7873	8282	6209	-
% of total area	17.30	21.08	19.48	35.39	28.11	34.67	49.42	42.17	-
DISSOLVED MANGANESE IN ELECTROLYTE [$\mu g/cm^2$]									
	2.14	3.23	4.91	7.74	8.32	9.73	12.08	11.27	12.91

OCPs of the corrosion coupons plated with manganese dioxide were stable at $+585(\pm 14)$ mV_{SCB} measured at pH 6.5 and $[Mn^{2+}] = 1$ mM. XPS spectra obtained from the plated coupons did not match any of the standard manganese spectra. Using a two peak model to fit the spectra of the plated manganese revealed a major peak at 49.89 eV and a secondary peak at 49.04 eV representing 84% MnO_2 and 16% $MnOOH$. To simulate the cathodic behavior of the manganese dioxide in a corrosion situation, a cathodic current was passed through the steel/deposit/water interface transferring charges ranging from 3.6 to 32.4 mC/cm². Figure 2 shows XPS spectra for the Mn3p orbital obtained from the reduced samples. The last sample, reduced by passing 32.4 mC, did not show any manganese and is not shown in Figure 2. A two peak model was used to fit the curvature of the Mn3p peaks. Table 3 illustrates the position and shape parameters resulting from the peak fitting.

The total area under the two peaks decreases with transferred charge, while the area ratio between the iron and the manganese peak increases (see Figure 2). The concentration of dissolved manganese in the electrolyte, shown in Table 3, increases during the reduction. We conclude that manganese is lost from the deposit. The only soluble manganese compound within the applied pH and potential range is divalent manganese, Mn^{2+} , thus the reaction (2) must have occurred.



$$E^0 = 1.315 \text{ V} \quad (2)$$

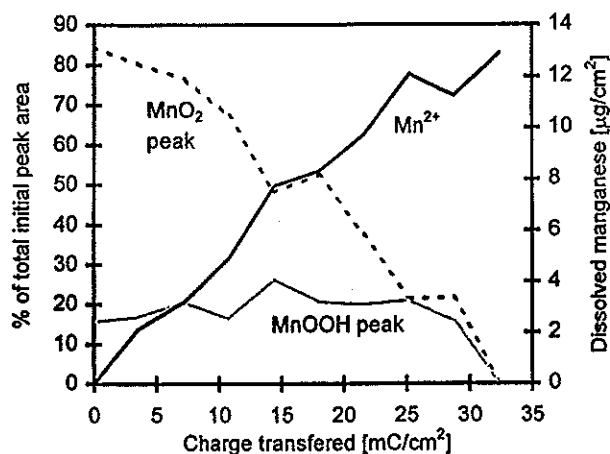


Figure 3. Mass balance for manganese during electrochemical reduction of manganese dioxide film.

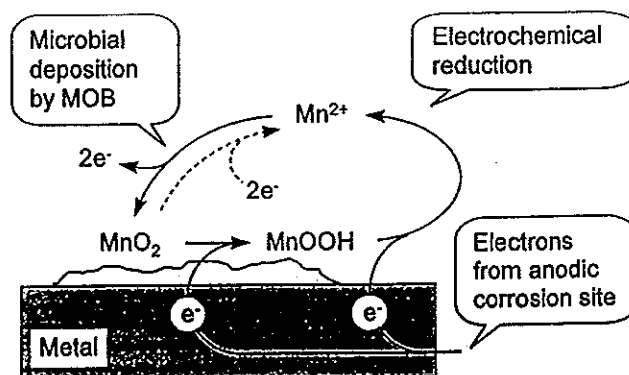
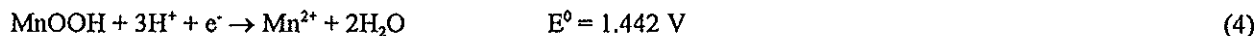
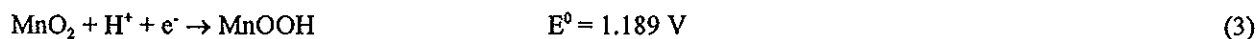


Figure 4. Manganese cycling at a metal surface including microbial oxidation/reduction and electrochemical reduction.

The total peak area decreases (due only to a decrease of the peak representing manganese dioxide) while the peak for MnOOH increases slightly. Figure 3 shows the relative area under the two peaks as well as the dissolved manganese as a function of transferred charge. The MnOOH is removed from the surface when all the MnO₂ is reduced. We conclude that the reaction of dissolving manganese dioxide occurs in two steps: 1- reducing MnO₂ to MnOOH (3) and 2- reducing MnOOH further to Mn²⁺ (4).



The first part of the reaction, reducing manganese dioxide to manganese oxyhydroxide, is identical to that proposed by Dickinson et al.^{13,14}. However, our results indicate that the end product of the reaction is dissolved divalent manganese, therefore, step 2 the reduction of MnOOH to Mn²⁺ must have occurred. The overall reaction, reducing manganese dioxide to divalent manganese, is similar to the mechanism of ennoblement proposed by Linhardt^{10,11}.

The cathodic properties of manganese dioxide on passive metals may initiate pitting corrosion. Passive metals often form a large number of metastable pits, that quickly repassivate again and therefore do not cause active corrosion of the metal. The biomined manganese dioxide, being a cathodic reagent and located at the surface of the metal, could postpone the repassivation of the pits and thus increase the possibility of active corrosion pits.

The end product, divalent manganese, can be mineralized again by the biofilm of manganese oxidizers. Thus, the amount of cathodically active manganese dioxide available in a corrosion process is only limited by the rate of biomined manganese. A schematic representation of the manganese cycle at a passive metal surface, including biomined manganese and electrochemical reduction of manganese dioxide is shown in Figure 4. It is possible that bacteria capable of reducing manganese oxides may be active as well. Consequently, the reduction of manganese dioxide may be a competition between biological and electrochemical pathways.

CONCLUSIONS

- 1) Minerals deposited by the manganese oxidizing bacterium *Leptothrix discophora* SP-6 consist of manganese dioxide, MnO₂.
- 2) The reduction of manganese dioxide occurs in two steps: manganese dioxide is first reduced to manganese oxyhydroxide, then to divalent manganese.
- 3) Biomined manganese may increase the corrosion rate of stainless steels by increasing the cathodic activity at the metal surface.

ACKNOWLEDGEMENT

This work was supported by the Faculty of Engineering and Science, Aalborg University, Denmark, the United States Office of Naval Research under the AASERT program, contract number N00014-92-J-1966, under ONR contract number N00014-95-1-0900, and by Cooperative Agreement BEC-8907039 between the National Science Foundation and Montana State University, Bozeman, MT, USA.

REFERENCES

1. A. Mollica, A. Trevis, "Correlation Entre la Formation de la Pellicule Primaire et la Modification de la Cathodique sur des Aciers Inoxydables Expérimentés en eau de Mer aux Vitesses de 0,3 A 5,2 m/s", Proc. 4th Int. Cong. Marine Corrosion and Fouling, (Juan-Les-Pins, Antibes, France, 1996).
2. R. Johnsen, E. Bardal, Corrosion 41, 5(1985): p. 296.
3. S. C. Dexter, G. Y. Gao, Corrosion 44, 10(1988): p. 717.
4. S. Motoda, Y. Suzuki, T. Shinohara, Corrosion Science 31(1990): p. 515.
5. M. Eashwar, S. Maruthamuthu, S. Sathiyarayanan, K. Balakrishnan, Corrosion Science 37, 8(1995): p. 1169.

6. V. Scotto, R. Di Cintio, G. Marcenaro, *Corrosion Science* 25, 3(1985): p. 185.
7. R. Holthe, E. Bardal, P. O. Gartland, "The time dependence of cathodic properties of stainless steels, titanium, platinum and 90/10 CuNi in sea water," *CORROSION/88*, Paper No. 398, (Houston, TX: NACE International, 1988).
8. B. Little, P. Wagner, F. Mansfeld, *Int. Mat. Rev.* 36, 6(1991): p. 253.
9. M. Eashwar, S. Maruthamuthu, *Biofouling* 8(1995): p. 203.
10. P. Linhardt, *Werkstoffe und Korrosion* 45(1994): p. 79.
11. P. Linhardt, in: E. Heitz, H. -C. Flemming and W. Sand (eds.), *Microbially Influenced Corrosion of Materials*, (Springer Berlin Heidelberg, 1996), p. 221.
12. W. H. Dickinson, F. Caccavo Jr., Z. Lewandowski, *Corrosion Science* 38, 8(1996): p. 1407.
13. W. H. Dickinson, Z. Lewandowski, *Biofouling* 10, 1-3(1996): p. 79.
14. W. H. Dickinson, F. Caccavo Jr., B. H. Olesen, Z. Lewandowski, *Applied and Environmental Microbiology*, 63, 7(1996): p. 2502.
15. W. H. Dickinson, Z. Lewandowski, "Manganese Biofouling of Stainless Steel: Deposition Rates and Influence on Corrosion Processes," *CORROSION/96*, Paper No. 291, (Houston, TX: NACE International, 1996).
16. D. Emerson, W. C. Ghiorse, *Applied and Environmental Microbiology* 58, 12(1992): p. 4001.
17. R. L. Gherna, in P. Gerhardt (ed.), *Manual of Methods for General Microbiology*, (American Society for Microbiology, Washington, 1981).
18. R. Giovanoli, U. Leuenberger, *Helv. Chem. Acta* 52(1969): p. 2333.
19. C. A. Johnson, A. G. Xyla, *Geochimica et Cosmochimica Acta* 52(1991): p. 2861.
20. P. Brewer, D. Spencer, *Limnol. Oceanogr.* 16(1971): p.107.
21. A. J. Bard, R. Parson, J. Jordan, "Standard Potentials in Aquatic Solutions", (Marcel Dekker, Inc., New York, 1985).

